The iron bars from the 'Gresham Ship': employing multivariate statistics to further slag inclusion analysis of ferrous objects

Thomas Birch and Marcos Martinón-Torres

ABSTRACT: An assemblage of post-medieval iron bars was found with the Princes Channel wreck, salvaged from the Thames Estuary in 2003. They were recorded and studied, with a focus on metallography and slag inclusion analysis. The investigation provided an opportunity to explore the use of multivariate statistical techniques to analyse slag inclusion data. Cluster analysis supplemented by principal components analysis revealed two groups of iron, probably originating from different smelting systems, which were compared to those observed macroscopically and through metallography. The analyses reveal that the bars were formed from raw blooms, and all were made with iron produced by the direct process. The outward uniformity of the bars is at odds with the variable quality of iron displayed within and between bars.

Introduction

In 2003 the Princes Channel wreck was salvaged from the Thames estuary. This wreck has been identified as an armed merchant ship built from English oak that was felled around 1574, tentatively linked to the merchant Thomas Gresham (Auer and Frith 2007; Wessex Archaeology 2005). Some 40 iron bars were salvaged from the hull area of the ship, along with lead and tin ingots, although it is thought that a great deal more was recovered during the 19th century. With concern over the future conservation and storage of these bars and little recording, the importance of their study cannot be underestimated.

This study presents the first results on the 17 iron bars which were available for study. Besides the macroscopic characterisation of the bars, this paper investigates the types of iron and iron alloys present, their purity and technological origins. The tentative date of the bars places them in a period where two ironmaking methods co-existed in Europe: the traditional direct or bloomery process, whereby ores rich in iron oxides are reduced to a metallic mass or 'bloom' in the solid state; and the new indirect method, based on blast furnaces operating at higher temperatures, whereby liquid, carbon-rich cast iron is obtained, which may be decarburised in a subsequent stage in order to make it malleable. Identifying the technological origin will provide an invaluable insight into the production of bar iron during this period, for which very little in the way of physical remains exists.

The study also identified compositional groups based on the analysis of slag inclusions (SI) entrapped in the metal. The last few decades have witnessed much discussion and analytical work on SI (Buchwald and Wivel 1998; Elban and Goodway 2003; Hedges and Salter 1979; Mackenzie and Whiteman 2006; Rostoker and Dvorak 1990; Sigurðardóttir 2004; Starley 1999; Tholander 1989; Williams 1990). More recently, methods have been developed in SI studies relating them to ore deposits, smelting and post-smelting processes, and in discussions of 'provenance' (Blakelock *et al* 2009; Coustures *et al* 2003; Desaulty *et al* 2008; 2009; Dillman and L'Héritier 2007). Whilst statistical methods have been employed in SI analysis, the potential of multivariate analysis in

defining groups has been little explored since the initial work by Hedges and Salter (1979). This investigation draws on recent work into non-reduced compound (NRC) ratios and aims to highlight the contribution multivariate statistics may have when applied to SI studies. NRC are compounds that pass from the ore into the slag (and slag inclusions), rather than passing into the metal phase (reduced compounds).

By combining typological, metallographic and SI information, we also aim to offer preliminary discussion on standardisation and quality control in the production and trade of iron in the post-medieval period.

The assemblage

On initial inspection, the iron bars can be distinguished by one key feature – their shape (Fig 1). Bars 18 and 76 are distinctive, with a flattish rectangular cross-section (*c*30x80mm), compared to the other bars, which have a square cross-section (*c*40x40mm, sometimes tapering to *c*20x20mm). Those bars considered complete exhibit another characteristic that is shared by both types: multiple bends. Often there are two to four bends, or folds, so the iron forms a packed pile, or package. The folded length is often about 2m. When straightened out, the bars would be either 4m or 6m, and the 6m bars weighed around 60kg.

Figure 1: Photographs and illustrations comparing the two different bar types: flattish rectangular cross-section (bar 18, right), square cross-section (bar 42, left).

The square-sectioned bars have a surface that undulates uniformly. These 'waves' repeat every 40–60mm, which suggests the use of a water-powered hammer, as such shaping would be extremely labour intensive to produce by hand. These are well attested historically and archaeologically in forges during the later medieval period in Europe (Awty 2006, 136; 2008; Hayman 2005, 18; van Laun 1979, 57–9; Smith 1997, 37). The hammer must have had a flattish head with slightly rounded edges in order to create such marks, which would be consistent with a relatively rapid drawing of the iron under the hammer head. These hammer marks were visible in X-radiographs underneath the corrosion products, especially at the bends where it appears that the bar was hammered thin for easier folding. The uniform surface and absence of any visible hammer indentations on the two flat iron bars (18 and 76) raises the possibility that these bars were rolled. This suggestion may also be supported by the definite lamellae and distorted grains visible in the microstructure of these bars, which appears to show a highly regular deformation process. A summary of the macroscopic observations along with the metallographic study can be seen in Table 1.

Methodology

Analytical protocol

One sample was obtained from each bar using a rotary angle grinder with a silicon carbide abrasive disc. Two samples were removed from bar 78, and none was taken from bar 39. Each section was then sub-sampled using a tile cutter to remove the areas potentially most affected by the annealing effect of the angle grinder, and the specimens were prepared as standard polished metallographic blocks. Caution is needed when extrapolating results from one sample for the whole bar stock, however the library of specimens allow for some general comments to be made.

The composition of the SI was determined using an Oxford Instruments energy dispersive spectrometer coupled to a JEOL JXA 8600 superprobe (EPMA-EDS), operating at 20kV with a processing time of 5 (INCA software arbitrary units) and ~40% deadtime. The metal phase was analysed using a wavelength dispersive spectrometer on the same instrument (EPMA-WDS). The calibration of the superprobe was based on pure elements and simple compounds. Analytical precision and accuracy of the measurements were monitored

Table 1: Summary table of macro- and microscopic information forthe iron bars.

Group	Bar	Section	Folds	Length (cm)	Unfolded (cm)	Weight (kg)	Features	Macro	Micro	Carbon	SI
A	43	sq	1	188	372	42.0	ham	W	fe (eq)	het	sgl
A	44	sq	1	193	569	70.0	ham	W, L	fe (dist)	het	sgl
A	47	sq	1	190	381	40.5	ham	W	fe (eq)	het	mlt
B	40	sq	2	203	512	56.5	ham	W	fe (eq)	het	sgl
B	42	sq	3	184	565	55.0	ham	S	fe (eq)	het	sgl mlt
B	45	sq	3	201	563	65.0	ham	S	fe(eq)+per.	het	mlt
B	78	sq	3	183	554	52.0	ham	S, W	hyper	none	sgl mlt
C	18	flat	2	197	425	60.0	rolled?	W, L	fe (eq)	min	sgl mlt
C	76	flat	2	188	415	65.0	rolled?	L	fe (eq)	het	sgl
frag	17	sq	-	160	160	9.0	ham	W, L	fe (eq)	het	sgl mlt
frag	22	sq	1	191	191	60.0	ham	-	fe (eq)	het	sgl
frag	30	sq	-	98	100	3.0	ham	S	fe (dist)	het	sgl
frag	38	sq	-	88	87	3.5	ham	W, L	fe (eq)	het	sgl
frag	39	sq	-	104	104	7.0	ham	-	-	-	-
frag	46	sq	1	181	287	28.0	ham	W, L	fe (eq)	het	sgl mlt
frag	48	sq	-	108	108	5.5	ham	W, S	fe (eq)	het	sgl mlt

Notes: macrostructure = macro; microstructure = micro; fragment = frag; square = sq; hammered = ham; weld-lines = W; lamellae banding = L; slag rich = S; equiaxed ferrite = fe(eq); distorted ferrite grains = fe(dist); interstitial pearlite = per; hypereutectoid structure = hyper; heterogeneous distribution = het; single-phased SI = sgl, multi-phased SI = mlt.

through repeated analysis of relevant certified reference materials. These were the three US Geological Survey basalts (BIR-1, BHVO-2 and BCR-2), as well as the British Chemical mild steel standard (B.C.S. No. 272 (S.S. No. 12)). For SEM-EDS, minor elements can be detected and quantified for amounts over 0.3wt%. The relative quantification error for minor element oxides (<1wt%) was around 10–15%, and for major element oxides (>1wt%) it was around 3%, except for soda which was marginally higher on some analyses. For EPMA, elements can be detected and quantified for amounts over 0.01wt%, but more accurately for concentrations above 0.1wt% (where soda and magnesia were more notably underestimated). Oxygen was not measured, but was calculated based on stoichiometry.

A minimum of 30 SI were analysed using EPMA-EDS area scans at different sites of interest for each sample. Only inclusions greater than 15µm diameter were analysed in order to reduce localised concentration effects (Dillman and L'Héritier 2007, 1815). Each SI was recorded for its location, shape, size, number and type of phases present, so that their information could be combined with observations made through optical microscopy.

The samples were etched with a 2% nital solution and examined under an optical microscope for a further assessment of the microstructure, carbon content and technological history of the metal.

Data processing

The methodology adopted here closely follows recent work on SI (Blakelock *et al* 2009, Dillman and L'Héritier 2007, Desaulty *et al* 2009), but explores the data differently, using multivariate statistics.

As in previous studies, initial data analysis exploration involved the use of bivariate plots of different NRC, to assess correlations between different oxides within and between samples. While a correlation matrix can serve the same purpose, the use of graphs also allows the identification of potential groups. Linear models were used for the plotting of data, but it was not considered necessary that the best fit line pass through zero, as this assumes that when one oxide is present, the other should be too. The linear model was not 'cleaned' to exclude outliers, for reasons already discussed (Blakelock *et al* 2009, 1748), but also because the inclusion of censored data may be informative statistically (Baxter 2003, 121). The *t*-test is only employed here when appropriate, that is when the data are normally distributed, and when a sample indicates relatively little internal variability (as the SI can then be compared collectively for their means). The differences between samples was judged based on linear relationships between certain com-

pounds (regression coefficient), the similarity of lines of best fit, as well as the distribution of outliers (residuals).

Hierarchical cluster analysis (HCA) is used here as a polythetic divisive method to generate multiple levels of grouping at different levels of similarity (Ward's method). This technique is further supplemented by standard principal components analysis (PCA) to characterise the groups and their associated variables. This analysis was specifically concerned with the subcompositional data for NRC (Na_2O, MgO, Al_2O_3, SiO_2, K_2O, CaO, TiO_2, MnO and BaO), and the variables employed were oxide ratios obtained by dividing each NRC concentration by the total sum of the subcomposition. Normalised subcompositions improve comparability between samples by removing the dominant variable (ie FeO), which would otherwise dilute all the others and dominate any statistical analysis. When discussed in the text, these ratios will be noted with an asterisk (eg SiO_2*) to differentiate them from the absolute oxide values (eg SiO_2).

PCA and cluster analysis should roughly tell the same story, as PCA supplements cluster analysis (Shennan 1997, 295) by revealing what characterises a cluster of cases. It also identifies which variables define the relationship between clusters, in terms of the covariance and correlation between the variables being analysed. The use of 'proportional data' (ie adds up to 100%) in PCA and other data-reducing statistical methods has been criticised theoretically, for when one major component is increased another component is directly affected and has to decrease. To mitigate against this issue, also known as 'closed data', statisticians have implored the use of data transformations. Data transformations, such as using the square root or standard log of data, 'open' up the dataset and free it from the closure constraint, allowing PCA to be conducted in a manner that is sounder theoretically. There are many forms of data transformation available; however it has also been argued that such transformations may distort the original dataset. It is not within the scope of this paper to detail the 'the closure problem' (Aitchison *et al* 2002, 296), nor the debate concerning 'standard PCA' versus logratio analysis (Aitchison *et al* 2002; Tangri and Wright 1993). Suffice to say, this analysis adopted standardised data, rather than un-standardised logged data, or ranked data, as they often 'give rise to similar results' with 'a similar substantive interpretation' (Baxter 2003, 78).

Slag Inclusions

The average compositions of SI for each bar are presented in Table 2. The EPMA analyses of the metal phase are presented as averages for each bar in Table 3.

Phosphorous and the Direct Process

Several scholars have attempted to address the issue of identifying the technological origin of iron. No consensus has been reached regarding how this can be achieved, but general observations have been made that

Table 2: Normalised average SEM-EDS results from the analysis of SI in the iron bars. The results are expressed as oxides (stoichiometrically) in wt% and the 'total' column provides average analytical total prior to normalisation.

Bar	n=	Na_2O	MgO	Al_2O_3	SiO_2	P_2O_5	SO_3	K_2O	CaO	TiO_2	MnO	FeO	BaO	Total
17	30	0.4	1.0	3.1	30.6	0.4	0.3	2.5	2.6	0.1	2.7	56.3	nd	103.1
18	40	0.6	1.1	4.0	27.6	bd	nd	2.6	2.8	0.1	3.3	58.0	nd	105.7
22	30	0.3	2.5	2.9	30.4	0.5	0.9	2.3	3.7	bd	15.0	41.2	0.4	103.6
30	31	0.3	3.3	3.3	41.3	0.0	0.5	3.7	4.9	0.1	18.4	23.4	0.8	102.0
38	30	0.8	2.5	7.2	47.3	0.2	0.2	5.6	6.1	0.3	4.4	25.5	nd	103.7
40	31	0.7	2.0	6.2	44.0	0.3	0.2	4.4	5.2	0.2	3.9	32.9	nd	102.8
42	31	0.3	0.9	2.8	31.7	0.5	0.2	2.4	2.2	0.1	2.4	56.5	nd	101.9
43	30	0.3	2.0	5.0	44.6	0.1	0.2	4.3	6.3	0.2	17.5	18.6	0.7	102.1
44	30	0.6	1.6	4.7	35.2	0.5	0.2	3.7	4.3	0.2	4.2	44.8	nd	102.3
45	31	0.3	0.9	3.9	28.9	0.6	0.2	1.9	3.7	bd	2.2	57.4	nd	102.4
46	30	0.7	2.5	7.2	52.0	0.2	bd	6.0	6.4	0.3	3.8	20.8	nd	102.2
47	30	0.4	1.2	4.8	29.7	0.6	0.1	3.2	3.6	0.1	3.3	53.1	nd	102.7
48	30	0.5	1.8	6.5	37.9	0.2	0.2	4.6	5.4	0.2	3.7	39.0	nd	100.9
76	30	0.4	1.1	3.8	33.9	0.6	0.1	3.2	3.1	0.1	3.3	50.4	nd	101.8
78 i	30	0.7	2.1	6.1	50.7	0.3	0.1	4.6	4.8	0.2	5.2	25.2	0.0	102.9
78 ii	30	0.5	1.2	3.9	30.3	0.4	0.0	2.6	2.9	0.0	3.9	54.1	0.0	101.2

Notes: below detection limits = bd; not detected = nd; number of analyses = n

Table 3: Raw EPMA data obtained from the analysis of the metal phase expressed as elements (wt%).

Bar	n=	Fe	Cl	Mn	Co	Ni	Cu	Zn	Sn	Pb	S	Si	Al	P	Ti	W	Mo	Cr	As	Total
17	5	100.229	0.008	0.016	0.090	nd	0.079	0.004	nd	0.068	0.007	nd	nd	0.043	0.003	0.017	nd	0.005	0.076	100.555
18	7	101.119	0.008	0.025	0.091	0.006	0.030	0.013	0.018	0.080	0.015	0.001	nd	0.018	0.004	0.025	nd	0.007	0.035	101.391
22	10	98.993	0.009	0.027	0.106	0.013	0.033	0.013	0.007	0.075	0.062	nd	nd	0.034	0.006	0.026	nd	0.005	0.043	99.373
30	5	98.338	0.008	0.026	0.083	0.007	0.035	0.007	0.018	0.051	0.010	nd	0.005	0.019	0.007	0.034	nd	0.006	0.039	98.617
38	10	99.880	0.004	0.013	0.091	0.011	0.030	0.010	0.008	0.053	0.007	nd	0.002	0.048	0.006	0.045	0.015	0.008	0.078	100.201
40	5	99.987	0.004	0.043	0.100	0.013	0.014	0.004	0.008	0.079	0.009	nd	nd	0.036	0.003	0.010	nd	nd	0.183	100.317
42	10	100.160	0.007	0.011	0.092	0.013	0.042	0.019	0.013	0.080	0.010	nd	nd	0.029	0.004	0.028	0.019	0.007	0.039	100.556
43	5	99.906	0.025	0.038	0.094	0.008	0.020	0.015	0.007	0.095	0.007	nd	0.004	0.010	0.007	0.019	nd	0.002	0.032	100.205
44	5	99.514	0.008	0.023	0.084	nd	0.034	0.010	0.006	0.092	0.012	nd	nd	0.028	0.003	0.013	nd	0.007	0.078	99.853
45	5	99.032	0.009	0.015	0.089	0.002	0.018	0.003	0.002	0.073	0.019	nd	nd	0.018	0.007	0.035	nd	0.006	0.050	99.326
46	10	99.930	0.008	0.012	0.102	0.007	0.053	0.016	0.005	0.066	0.003	nd	nd	0.040	0.004	0.018	0.017	0.009	0.034	100.214
47	10	100.576	0.010	0.014	0.096	0.010	0.037	0.016	0.003	0.091	0.007	nd	nd	0.027	0.006	0.043	0.002	0.007	0.053	100.884
48	5	98.606	0.011	0.009	0.087	0.006	0.023	0.019	0.022	0.047	0.009	nd	nd	nd	0.004	0.012	nd	0.007	0.122	98.874
76	5	98.316	0.007	0.018	0.086	0.010	0.144	0.012	0.012	0.074	0.002	nd	nd	0.066	0.002	0.030	nd	0.003	0.041	98.745
78i	10	99.842	0.006	0.012	0.094	0.005	0.115	0.016	nd	0.059	0.007	nd	nd	0.069	0.008	0.033	0.014	0.005	0.058	100.243

Notes: below detection limits = bd; not detected = nd; number of analyses = n.

appear to distinguish bloomery iron (direct process) from wrought iron (indirect process). Hedges and Salter (1979) based their observations on certain compounds that reduce more easily depending on furnace conditions, whilst Tholander (1989) focused more on inclusion morphology (phases) to distinguish processes. Rostoker and Dvorak (1990) implemented 'discrimination limits' of certain oxides, but accept that more data are needed to characterise the differences. Others have sought to discriminate between processes based on SI composition and type (Buchwald and Wivel 1998; Gordon 1997; Mackenzie and Whiteman 2006; Starley 1999; Williams 1990). More recently, Dillmann and L'Héritier (2007) have presented a methodology based on the analysis of SI that potentially allows the differentiation between iron produced by the direct and indirect methods. The latter bear SI that are richer in phosphorous and poor in alumina and alkali earth oxides relative to iron, contrasting with the opposite pattern for SI in bloomery iron.

When the data from the Princes Channel ship bars are plotted, it becomes obvious that we are dealing with bloomery iron in all cases (see Fig 2). The phosphorous contents in the SI of the bars are relatively low in all cases. None of the SI in bar 18 contain any phosphorous, and bars 30 and 43 have very few SI containing phosphorous, whilst less than half the analyses in several other bars detected phosphorous. The average weight percent of the oxide in all the SI is not higher than 1% for any the bars.

The identification of these bars as the product of the direct process is of interest for technical reasons, as their construction would have required the welding of several blooms, but also in the light of their relatively late date. As they were loaded onto a ship dated *post quem* to 1574, it seems reasonable to assume that the bars date to the

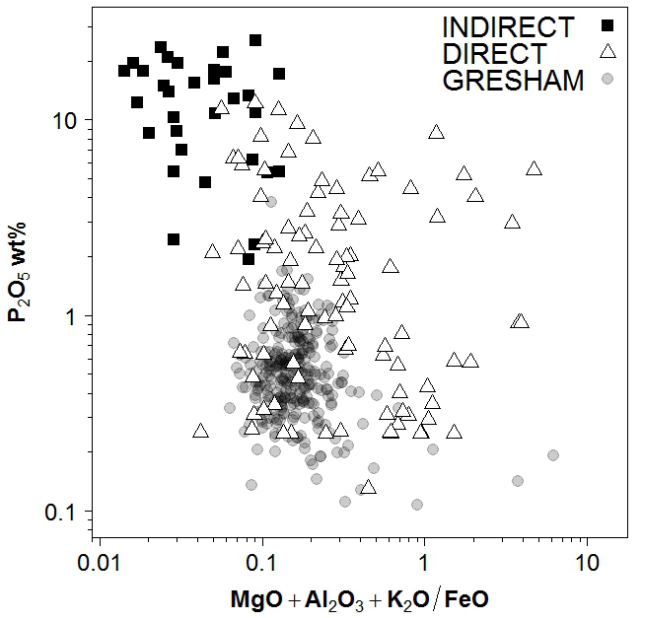

Figure 2: Bivariate scatterplot distinguishing the direct and indirect processes based on the ratio of phosphorous pentoxide to the weighted contents of several other compounds. Data provided by Philippe Dillman, on which the Gresham SI have been plotted as transparent markers to illuminate point density in the region of the direct process (axes log-scaled to improve visibility of datapoints).

late 16th-century or possibly later. By this period, the indirect process was increasingly established in large parts of Europe (King 2005; Pipping 1982; Tylecote 1976; 1987; 1991), so the smelting technology used is of relevance when assessing the likely origins and broader economic and technological contexts where these bars would have been produced and traded.

Multivariate statistics – defining Group I and Group II

The cluster analysis of the SI data revealed two distinct groups: one including all the SI for bars 22, 30 and 43 (Group I), and the other one including all the other bars (Group II). No correspondence was found between these SI groups and the typological groups defined macroscopically. It is only through further statistical inference that we can understand the causes of this grouping, by supplementing the technique with PCA (Figs 3 and 4).

In the PC space, Group I is characterised by a higher proportion of MnO*, BaO* and MgO* relative to SiO_2*. In particular, the average values for MnO* are four to five times higher in Group I than in Group II (MnO is 17.4% for Group I and 3.6% for Group II). Assuming that the levels of MnO are practically negligible in clay and fuel ash, the significantly higher levels of this oxide in Group II demonstrate that a different ore or ore mixture is likely to have been one of the main parameters differentiating both smelting systems. These three bars are often distinguished from the main corpus by other NRC ratios. Two bars (22 and 40) were chosen to represent the two groups described, and a *t*-test comparing their means confirmed that their NRC ratios (SiO_2/MnO, CaO/MgO and K_2O/MgO) are indeed significantly different (Table 3; cf Blakelock *et al* 2009).

Group II is the larger group and has a greater continuum of chemical diversity, which it is not possible to subdivide easily by HCA or PCA. Compared to Group I, the SI in this group display higher proportions of K_2O, Al_2O_3, Na_2O and SiO_2, with variable amounts of CaO and TiO_2. Further variation within this group appears in the SO_3 and P_2O_5 levels, although these are generally very low (<0.5%).

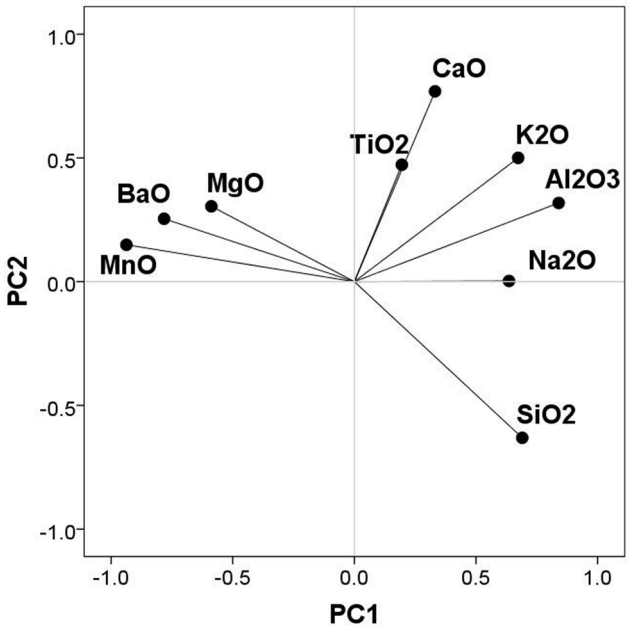

Figure 3: PCA loading plot of the NRC variables. Variance explained: PC1: 44.7%; PC2: 19.4%; PC3: 10.7%..*

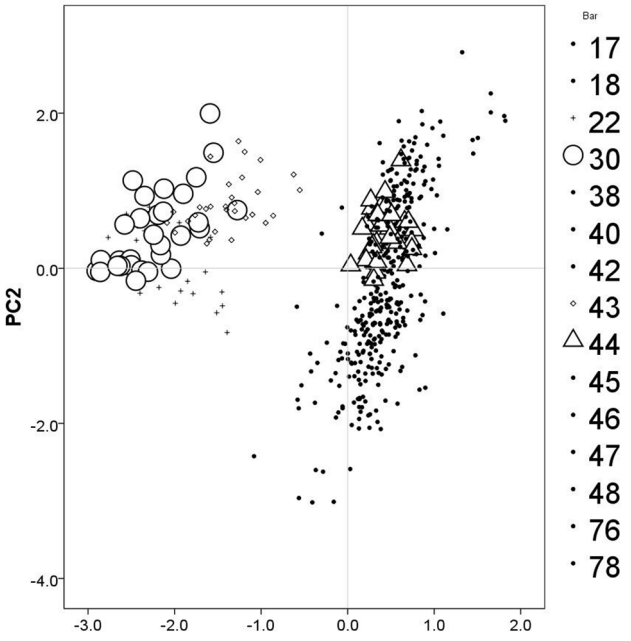

Figure 4: PCA plot of the subcomposition of NRC of the SI in the bars analysed, where Groups I and II can be clearly differentiated. SI for two bars (30 and 44) are highlighted to exemplify the relatively tight compositional subgroups each bar forms (ie specific blooms) within the broader groups (ie smelting systems). Variance PC1: 44.7%; PC2: 19.4%; PC3: 10.7%..*

Table 4: Results from three t*-tests of NRC ratios comparing means between bars 22 and 40.*

	SiO_2/MnO			CaO/MgO			K_2O/MgO		
	t	df	p	t	df	p	t	df	p
Two independent samples compared: bar 22-S3 and bar 40-S2.	-14.062	30.046	0	-21.222	44.693	0	-20.418	57.953	0

Notes: t-value =t; degrees of freedom = df; and probability = p

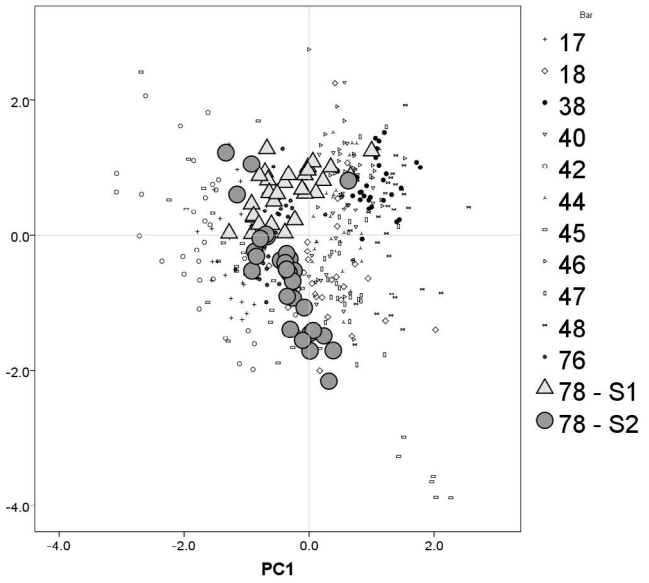

Figure 5: PCA of the NRC of the SI in Group II bars, with SI for the two sections of bar 78 highlighted. Note their slight separation, indicative of the existence of two different blooms welded to form the bar. Variance explained: PC1: 44.5%; PC2: 17.4%; PC3: 14.0%..*

Even though all the bars in Group II form a relatively continuous cluster, an interesting pattern is noticeable when the SI in the PC plot are marked by sample number. With very few exceptions, the SI for each sample cluster relatively tightly, marginally overlapping with other bars but still showing significant internal coherence that singles out each bar (although this is difficult to show in a black and white image, some examples are illustrated in Figure 5). The internal SI chemical homogeneity per bar is a strong indication that each bar section represents a raw bloom, all of them from the same smelting system, but showing slight differences between smelts. This impression is corroborated in the analysis of bar 78, from which two samples were taken at different points of its length: the plots of SI for those two sections overlap each other and the rest of Group II, but still show clearly that they form two chemical subgroups originating from two blooms that were welded into the same bar (Fig 5). This overall pattern indicates that the bars were made by welding raw blooms from the same smelter, while leaving scope for discussion of how different ratios may reflect variation in skill, efficiency or other engineering parameters between smelting batches. An open question, however, is whether Group I and II would represent two different smelters or simply the use of two different ore charges (see Charlton *et al* 2010).

Metallography

A summary of the metallographic study can be found in Table 1, which describes the predominant macrostructural features, microstructural phase and SI type. The bulk of the iron bars studied are dominated by ferrite grains, consistent with raw bloomery iron (see Figure 6 for examples of the metallographic sections). However, a great deal of heterogeneity is noticeable both within and between bars, denoting a lack of standardisation. Except for the specimens from bars 22, 45 and 76, distinctive weld lines were identified in all the bars. These appear to

Figure 6: Metallographic sections of different bars, exemplifying their internal heterogeneity. From top to bottom: 17, 18 and 78 (reflected light, 2% nital, image widths = 2mm).

be intrinsic to the iron in the form of large slag stringers surrounded by diffuse carbon regions. Many of the bars show high-carbon regions and localised hypereutectoid regions, as well as areas of ferrite with interstitial pearlite. This heterogeneous distribution, along with their prevalence near SI, indicates that the carburisation is primary from the smelt. The bars are generally rich in SI, with bars 17 and 42 containing a network of interconnected amorphous slag stringers ('vein-like' structure) characteristic of bloomery iron. Some of the bars contain distorted ferrite grains exhibiting no Neumann bands. Others, with their equiaxed ferrite grains, indicate that the bars were annealed long enough for partial and complete grain regrowth. The Widmanstätten structure, remnant in cases, seen in many of the specimens, and prevalent in bar 30, indicates that the bars were heated to high temperatures in the austenite temperature range (*c*850°C) followed by air cooling. Bars 42 and 76 have a clear hypoeutectoid layer with diffuse boundaries on their outer surface.

The different iron microstructures attest to variable smelting practices and degrees of working and refining. The carbon segregation and layered structure in some bars indicates a high degree of folding and welding of the iron bloom before being incorporated into the bar iron. The clear layered structure exhibited in some bars is formed by alternating layers of pure (fine and coarse) ferrite, and ferrite with pearlite, some layers defined by slag lines indicative of welds or folds. The fine ferrite grains in some layers may indicate a high degree of previous cold working before grain regrowth. The larger ferrite grains indicate low level deformation prior to annealing. A few of the bars (22, 45 and 76) contain comparatively fewer SI and show no weld lines, indicating a more refined stock.

A feature to be highlighted is the lack of correlation between the different microstructures and iron alloys identified during metallography, on the one hand, and the macroscopic or SI chemical groups. The only notable characteristic is that bars in Group I only contain single phased and two-phased (glassy containing wüstite) SI, compared to the multi-phased SI frequent in many of the other bars.

The EPMA-WDS analyses confirmed the SI and metallographic data, showing that the metal phase is a very pure iron, with around 0.1% Co trace consistent in every bar (occasionally detecting 1% Al). There is a trace of Cu present in some bars, reaching values above 0.1% for bars 18, 76 and 78, as well as traces of Pb and As. Phosphorous is detected inconsistently in the metal phase at trace level. This is similarly the case for Ti, which is also present in all SI. Given, however, the very low levels of all of these elements, around the detection limits of the instrument (~0.01%), it would be difficult to attempt any groupings based on the presence/absence or concentration of any of these elements.

Discussion and conclusion

This study has shown that the iron in all of the bars from the Princes Channel ship was smelted by the direct process, and that they were formed by welding raw blooms of rather heterogeneous stock. The internal variability and generally coarse quality of the iron seem in stark contrast with their standardised outward appearance, size and typology. This disparity, previously noted for Roman bar iron in France (Pagès *et al* 2008, 275), suggests that either the consumers to which this cargo was destined were not very discerning, quality control was not rigid or universal, the iron was not meant for high-quality applications, or that these bars simply do not represent the higher end of the spectrum in the European iron market.

From a methodological viewpoint, it was shown that the treatment of NRC data from SI by multivariate statistics can be of great use in identifying groups that may be related to different smelting systems. The same methodological approach may be useful in the future, when comparing smelting slag to SI data for provenance investigations (cf Blakelock *et al* 2009). Likewise, as the PCA reveals subtle compositional subgroups attributable to individual blooms, this approach may provide an indirect proxy to evaluate intra- and inter-smelt variation (cf Humphris *et al* 2009; Charlton *et al* 2010). For this case study in particular, the bars can be allocated to two distinct groups on the basis of the SI data, which are clearly related to different ore charges and, potentially, different producers. If the latter was true, then the bars would constitute indirect evidence of a separation between specialised smelters and smiths.

There is a great deal of information on the iron bar trade and references to Sir Thomas Gresham (eg Björkenstam 1982; Buchwald 2005; Cleere and Crossley 1985; Evans and Ryden 2007; Hart 1971; Hildebrand 1992; King 1996; 2003; 2005; Nef 1987; Tylecote 1962). Our ongoing research effort concentrates now on contextualising these finds in the broader technological and economic context of the growing international trade of iron in the post-medieval period, by investigating the origins and likely destination of this cargo.

Note

This paper was submitted in 2009, and thus it does not consider the growing number of publications on SI published since then, many of which complement the approaches taken here.

Acknowledgements

We are indebted to thank Peter Crew for his comments on the draft of this paper, and to Thilo Rehren for his guidance and discussion. We would also like to thank David Cranstone for providing helpful historical references, Maxime L'Héritier for bringing to our attention Pagès' work on Roman iron bars, and Philipe Dillman for providing experimental data. Many thanks are owed to Clive Orton, David Orton and Mike Charlton for fruitful and stimulating discussions on statistical treatment of data.

This work was undertaken as part of the Gresham Ship Project, a five year research programme co-ordinated by UCL and generously supported by the Port of London Authority. This study would not have been possible without the help and support of the following people and organisations: Dean Sully and Gustav Milne from UCL, also part of the Gresham Ship Project; Stavriani Orfanou and Ioannis Papadias (sampling and recording); Historic England, Fort Cumberland, Portsmouth (facilities); Kelly Domoney (X-radiography) and Simon Groom and Kevin Reeves (technical assistance at the UCL Wolfson Archaeological Science Laboratories).

References

Aitchison J, Barceló-Vidal C and Pawlowsky-Glahn V 2002, 'Some comments on compositional data analysis in archaeometry, in particular the fallacies in Tangri and Wright's dismissal of logratio analysis', *Archaeometry* 44(2), 295–304.

Awty B G 2006, 'The elusive Walloon finery forges of Liège', *Historical Metallurgy* 40(2), 129–37.

Awty B G 2008, 'The Austrian lift-hammer - its probable Walloon origin', *Historical Metallurgy* 42(1), 12–2.

Auer J and Firth A 2007, 'The 'Gresham Ship': an interim report on a 16th-century wreck from Princes Channel, Thames Estuary', *Post-Medieval Archaeology* 41(2), 222–241.

Baxter, M 2003, *Statistics in Archaeology* (London).

Blakelock E, Martinón-Torres M, Veldhuijzen H A and Young T 2009, 'Slag inclusions in iron objects and the quest for provenance: an experiment and a case study', *Journal of Archaeological Science* 36(8), 1745–57.

Björkenstam N 1982, ' Technology, production, costs', in G Pipping (ed), *Iron and Steel on the European Market in the 17th Century: a contemporary Swedish account of production forms and marketing* (Stockholm).

Buchwald V F 2005, *Iron and Steel in Ancient Times* (Copenhagen).

Buchwald V F and Wivel H 1998, 'Slag analysis as a method for the characterization and provenancing of ancient iron objects', *Materials Characterization* 40, 73–96.

Charlton M, Crew P, Rehren Th and Shennan S J 2010, 'Explaining the evolution of ironmaking recipes – an example from northwest Wales', *Journal of Anthropological Archaeology* 29, 352–367.

Cleere H and Crossley D 1985, *The Iron Industry of the Weald* (Leicester).

Coustures M P, Béziat D and Tollon F 2003, 'The use of trace element analysis of entrapped slag inclusions to establish ore-bar iron links: examples from two Gallo-Roman iron-making sites in France (Les Martyrs, Montagne Noire, and Les Ferrys, Loiret)', *Archaeometry* 45(4), 599–613.

Desaulty A-M, Dillman P, L'Héritier M, Mariet C, Gratuze B, Joron J-L and Fluzin P 2009, 'Does it come from the Pays de Bray? Examination of an origin hypothesis for the ferrous reinforcements used in French medieval churches using major and trace element analyses', *Journal of Archaeological Science* 36, 2445–2462.

Desaulty A-M, Mariet C, Dillman P, Joron J-L and Fluzin P 2008, 'A provenance study of iron archaeological artefacts by Inductively Coupled Plasma-Mass Spectrometry multi-elemental analysis', *Spectrochimica Acta Part B* 63, 1253–1262.

Dillman P and L'Héritier M 2007, 'Slag inclusion analyses for studying ferrous alloys employed in French medieval buildings: supply of materials and diffusion of smelting processes', *Journal of Archaeological Science* 34(11), 1810–1823.

Elban W L and Goodway M 2003, 'Inclusions in 19th-century American wrought iron structural cable wires', *Historical Metallurgy* 37(2), 106–19.

Evans C and Rydèn G 2007, *Baltic Iron in the Atlantic World during the eighteenth century* (Leiden).

Gordon C 1997, 'Process deduced from ironmaking wastes and artefacts', *Journal of Archaeological Science* 24, 9–18.

Hart C 1971, *The Industrial History of Dean* (Newton Abbot).

Hayman R 2005, *Ironmaking: the history and archaeology of the iron industry* (London).

Hedges R E M and Salter C J 1979, 'Source determination of iron currency bars through analysis of slag inclusions', *Archaeometry* 21(2), 161–75.

Hildebrand K-G 1992, *Swedish Iron in the Seventeenth and Eighteenth Centuries Export Industry before the Industrialization* (Stockholm).

Humphris J, Martinón-Torres M, Rehren Th and Reid T 2009, 'Variability in single smelting episodes – a pilot study using iron slag from Uganda', *Journal of Archaeological Science* 36, 359–369.

King P 1996, 'Early Statistics for the iron industry: a vindication', *Historical Metallurgy* 30(1), 23–46.

King P 2003, 'The iron trade in England and Wales, 1500–1815: the charcoal iron industry and its transition to coke', unpublished PhD thesis, University of Wolverhampton.

King P 2005, 'The production and consumption of bar iron in early modern England and Wales', *Economic History Review,* 57(1), 1–33.

van Laun V 1979, '17th century ironmaking in south west Herefordshire', *Historical Metallurgy* 13(2), 55–65.

Mackenzie R J and Whiteman J A 2006, 'Why pay more? An archaeometallurgical investigation of 19th-century Swedish wrought iron and Sheffield blister steel', *Historical Metallurgy* 40(2), 138–49.

Nef J U 1987, 'Mining and Metallurgy in Medieval Civilisation', in M M Postan and E Miller (eds), *The Cambridge Economic History of Europe* (Cambridge), 735–56.

Pagès G, Long L, Fluzin P and Dillman P 2008, 'Réseaux de production et standards de commercialisation du fer antiqueen Méditerranée: les demi-produits des épaves romaines des Saintes-Maries-de-la-Mer (Bouches-du-Rhône)', *Revue Archéologique de Narbonnaise* 41, 261–283.

Pipping G (ed) 1982, *Iron and Steel on the European Market in the 17th Century* (Stockholm), 200–260.

Rostoker W and Dvorak J 1990, 'Wrought irons: distinguishing between processes', *Archeomaterials* 4(2), 153–66.

Shennan S 1997, *Quantifying Archaeology* (Edinburgh).

Sigurðardóttir K H 2004, 'Provenance studies of iron from Iceland', in G Guðmundsson (ed), *Current Issues in Nordic Archaeology. Proceedings of the 21st Conference of Nordic Archaeologists 6-9 September 2001 Akureyri, Iceland* (Reykjavik), 119–124.

Smith T 1997, 'The Jernkontoret 250th anniversary conference', *Historical Metallurgy* 31(1), 36–41.

Starley D 1999, 'Determining the technological origins of iron and steel', *Journal of Archaeological Science* 26, 1127–33.

Tangri D and Wright R V S 1993, 'Multivariate analysis of compositional data: applied comparisons favour standard principal components analysis over Aitchison's loglinear contrast method', *Archaeometry* 35(1), 103–12.

Tholander E 1989, 'Microstructure examination of slags as an instrument for identification of ancient iron-making processes', in R Pleiner (ed), *Archaeometallurgy of Iron. International Symposium of the Comite´ pour la Siderurgie Ancienne de L'UISPP*, (Prague), 35–41.

Tylecote R F 1962, *Metallurgy in Archaeology* (London).

Tylecote R F 1976, *A History of Metallurgy* (London).

Tylecote R F 1987, *The Early History of Metallurgy in Europe* (London).

Tylecote R F 1991, 'Iron in the Industrial Revolution', in R F Tylecote and J Day (eds), *The Industrial Revolution in Metals* (London), 200–260.

Wessex Archaeology 2005, Princes Channel Wreck, Thames Estuary, Phase III Summary Report, unpublished report 57330.01.

Williams A R 1990, 'Slag inclusions in armour', *Historical Metallurgy* 24(1), 69–80.

The authors

At the time of writing, Thomas Birch was part of a two-year postdoctoral research project studying ancient coinage at the Institute of Archaeological Sciences at the Goethe University in Frankfurt am Main. He completed his PhD in the Department of Archaeology at the University of Aberdeen in 2013, where he investigated the provenance of iron weapons from Iron Age sites in Southern Scandinavia. His broad interest in early medieval metallurgy in NW Europe, particular in ferrous metallurgy, has led him to actively participate in researching evidence for metallurgy in Iceland.
Address: Goethe Universität Frankfurt am Main, Institut für Archäologische Wissenschaften, Abt. II, Norbert-Wollheim-Platz 1, 60629 Frankfurt am Main, Germany
Email: birch@em.uni-frankfurt.de

Marcos Martinón-Torres is Professor of Archaeological Science at the UCL Institute of Archaeology, where he co-ordinates an MSc in the Technology and Analysis of Archaeological Materials and supervises several research students working on ancient materials and technologies across the world. His research interests include material culture and technology, the applications of science to archaeological problems, and the interplay between archaeology, anthropology, science and history. Ongoing projects focus on Renaissance alchemy in Europe, pre-Columbian metallurgy in America, and the logistics behind the making of the Chinese Terracotta Army.
Addrress: Institute of Archaeology, University College London, 31-34 Gordon Square, London, WC1H 0PY, United Kingdom.
Email: mail: m.martinon-torres@ucl.ac.uk